

PERFORMANCE MEASURES OF UNDERWATER IMAGE ENHANCEMENT TECHNIQUES

Mr. M. KRISHNA KUMAR¹, P. THANALAKSHMI²

Assistant Professor, Dept. of Electronics and Communication Engineering, Grace College of Engineering, Tuticorin¹

PG Student, Dept. of Electronics and Communication Engineering, Grace College of Engineering, Tuticorin²

Abstract: Underwater images often suffer from color distortion and low contrast, because light is scattered and absorbed when travelling through water. Such images with different color tones can be shot in various lighting conditions, making restoration and enhancement difficult. There are several algorithms available which is helpful in restoring the underwater images back to the actual scene. In this project we analysis three different underwater image enhancement algorithms such as DSPV, AACP, G-GIF for restoring both the underwater images as well as videos. Also, the experimental results of these three algorithms are analysed for the better understanding of the performance. The image restoration aims to recover a degraded image using a model of the degradation and of the original image formation.

Keywords: Difference Structure Preservation Value, Graphical User Interface Development Environment, Adaptive Attenuation Curve Prior, Mean Square Error, Mean Square Error, Just In Time, Remotely Operated Vehicle.

I. INTRODUCTION

Technology advances in manned and remotely operated submersibles allow people to collect images and videos from a wide range of the undersea world. Waterproof cameras have become popular, allowing people to easily record underwater creatures while snorkeling and diving. These images or videos often suffer from color distortion and low contrast due to the propagated light attenuation with distance from the camera, primarily resulting from absorption and scattering effects. Therefore, it is desirable to develop an effective method to restore color and enhance contrast for these images. Even though there are many image enhancing techniques developed, such as white balance, color correction, histogram equalization, and fusion-based methods, they are not based on a physical model underwater, and thus are not applicable for underwater images with different physical properties.

Restoration of images

The image restoration aims to recover a degraded image using a model of the degradation and of the original image formation; it is essentially an inverse problem. These methods are rigorous but they require many model parameters and can be extremely variable.

Enhancement of images

Image enhancement is a technique of improving the quality of image by improving its feature and its RGB values. A major difficulty to process underwater images comes from light attenuation, it limits the visibility distance, at about twenty meters in clear water and five meters or less in muddy water. The light reduction process is caused by the absorption (which removes light energy) and spreading (which changes the direction of light wave path). Absorption of light and its scattering effects are because of the water itself and to other components such as dissolved organic matter or small observable floating particles. Due to this difficulty, underwater imaging suffers too many problems.

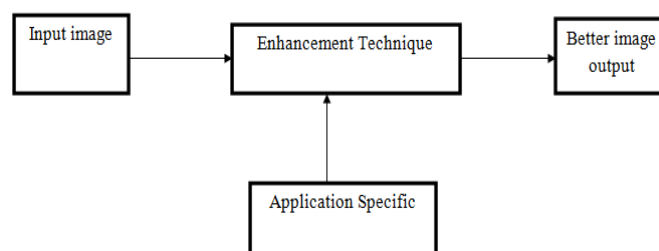


Figure 1: Basic block of Image Enhancement



Automatic station-keeping, involving motion estimation in order to maintain a fixed position, has been implemented for remotely operated vehicles with two and three degrees of freedom. Underwater images often suffer from color distortion and low contrast, because light is scattered and absorbed when traveling through water. Such images with different color tones can be shot in various lighting conditions, making restoration and enhancement difficult.

II SYSTEM DESIGN AND IMPLEMENTATION

Implementation of DSPV:

The implementation of DSPV algorithm to restore the underwater images required the following parameters to estimate:

- Estimation of Depth Map
- Restoration of Transmission Map
- Refine Transmission Map
- Estimation of Atmospheric Light
- Difference-Structure-Preservation Prior

Estimation of Depth Map

As the relationship among the scene depth d , the brightness v and the saturation s has been established and the coefficients have been estimated, the depth map of a given input hazy image can be restored according to Equation,

$$d(x) = \theta_0 + \theta_1 v(x) + \theta_2 s(x) + \varepsilon(x) \text{ Equation (4.1)}$$

where, x -position within the image,

d - the scene depth,

v - the brightness of the hazy image,

s - saturation,

$\theta_0, \theta_1, \theta_2$ - unknown linear coefficients,

$\varepsilon(x)$ - random variable.

The model tends to consider the scene objects with white color as being distant. Unfortunately, this misclassification will result in inaccurate estimation of the depth in some cases. Each pixel in the neighbourhood needs to be considered. Based on the assumption that the scene depth is locally constant, the raw depth map can be processed by:

$$d_r(x) = \min_{y \in \Omega_r(x)} d(x) \text{ Equation (4.2)}$$

where, $r(x)$ - an $r \times r$ neighbourhood centred at x ,

d_r - the depth map with scale r .

Restoration of Transmission Map

The restoration of transmission map for a single input haze image can be estimated by the equation given below,

$$t(x) = e^{-\beta d(x)} \text{ Equation (4.3)}$$

where, x -position of the pixel within the image,

t - medium transmission,

β - scattering coefficient of the atmosphere

d -depth of scene.

Refine Transmission Map

It is evident to suppress small variations through adjacent pixels. However, one may still obtain an inconsistent scene transmission for objects with large structural regions. To overcome this limitation and get a better transmission map, it is necessary to follow the idea described earlier of minimizing the cost function to obtain the refined $t(x)$.

$$\inf_{t \in R} E_t = u \|\hat{t} - t\|^2 + \mathcal{R}(t) \text{ Equation (4.4)}$$

Normally, images consist of various patterns and it is difficult to describe an image by one distribution. Fortunately, structural similarities are prevalent in natural images, which will be fully exploited to build the regularization $R(x)$.

Estimation of Atmospheric Light

As the depth map of the input hazy image has been recovered, the distribution of the scene depth is known. The Bright regions in the map stand for distant places. According to Equation below,

$$A = I(x), x \in \{x | \forall y : d(y) \leq d(x)\} \text{ Equation (4.5)}$$

Difference-Structure-Preservation Prior

First, to provide a method to measure the local depth consistency. In addition, to use the locally consistent depth as a regularize, one can assume that a local patch can be approximated by a sparse linear combination of elements from a neighbour basis set. More importantly, through building the difference-structure -preservation dictionary, the results have demonstrated that our approach is effective at restoring images. To this end, one can recast the problem as



finding a solution to transmission under scene constraints in the feasible range. Through the selection of parameters, an optimal transmission can be proposed and the complete calculation process is summarized.

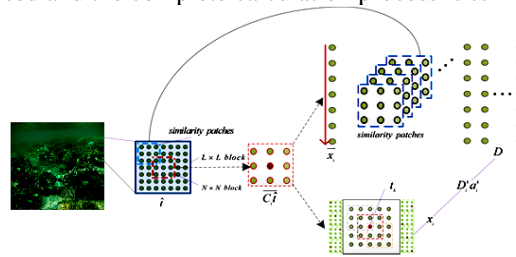


Figure2: The process of generating the training samples with DSPV

Spatiality Consistent Depth

The depth edge consistency is decided using neighbouring pixels. Hence, whether pixels lie on the same depth is decided only by the locations of the pixels. Following this idea, the pixel and its nearest neighbours as a vector variable can be modelled in order to measure the depth information. One can call this principle the local depth consistency. To determine whether there are other pixels at the same depth, one must need a set of neighboring training sample patches so that the transformation matrix can be calculated.

$$C_i^T \hat{t} = [\hat{t}_1, \hat{t}_2 \dots \hat{t}_s] \text{ Equation (4.6)}$$

where, s - the number of pixels in the image.

The vector contains all the components within the window $N \times N$. Then, use a $L \times L (L > N)$ training block to find the training samples. In this way, there is a matrix for each initial transmission patch x_i . Although there are many neighboring patches, it may lead to inaccurate estimation vector x_i and then produce misty results with high residual fog because sub-patches may not have the same depth.

Adaptive Attenuation Curve Prior

The non-local Haze-Line prior describes the change between the clear image J and the observed image I . However, in the underwater environment, the change is much more complicated to deal with. The reason is that dust-like particles in the medium lead to wavelength-dependent attenuation coefficients. The degeneration process for underwater images can be generally formulated as

$$I_c(x) = t_c(x) \cdot J_c(x) + (1 - t_c(x)) \cdot B_c, c \in \{r, g, b\} \text{ Equation (4.7)}$$

The transmission $t_c(x)$ depends on both the distance and wavelength. A more general prior, namely adaptive attenuation-curve prior, was proposed for various imaging environments, like haze, fog and water. It is important to define that pixels with similar colors belong to the same cluster towards a clear image. For the clear outdoor natural image, the work has verified that several hundred color clusters can represent all colors of the image with the acceptable result. Hence it is validated it on the BSDS300 dataset. Specifically, the K-means is used to find 500 clusters for each image and renewed every pixel value with its corresponding cluster center. The generated images had satisfactory PSNR with 36.6dB to 52.6dB. The observation is also valid for underwater images. In the underwater environment, there are two factors affecting the change between clear image and the observed image: the varying scene depth $d(x)$ from the camera to objects, which leads to the difference of transmission $t(x)$ for every pixel, and the wavelength-dependent attenuation coefficient β_c , which results in the difference of three elements in transmission vector, generating $t_c(x)$. Because of these two factors, the scene radiance $J_c(x)$ from the same cluster (with similar original colors) is attenuated in varying degrees, thereby generating different captured colors $I_c(x)$ in the observed image. The wavelength-dependent attenuation coefficient will bend the line into a power function curve. Therefore, it is named as an attenuation-curve.



Figure3: Four clusters' pixels in the clear Image and the corresponding clusters with different locations in RGB space.



Figure4: The synthetic image with the same clusters and the corresponding attenuation curves in RGB space.

Globally Guided Image Filtering:

To measure the local depth consistency, use the locally consistent depth as a regularize, Assume that a local patch can be approximated by a sparse linear combination of elements from a neighbour basis set. A simple single image haze removal algorithm is introduced by using the proposed G-GIF and the Koschmiedars law.

Flow Diagram of G-GIF:

The global atmospheric light $A_c (c \in \{r, g, b\})$ is empirically determined by using a hierarchical searching method based on the quad-tree subdivision. The value of the transmission map $t(p)$ is then estimated by using the proposed G-GIF. Finally, the scene radiance $Z(p)$ is recovered.

According to the Koschmiedars law, a haze image is generally modelled by:

$$X_c(p) = Z_c(p)t(p) + A_c(1 - t(p)) \text{ Equation (4.8)}$$

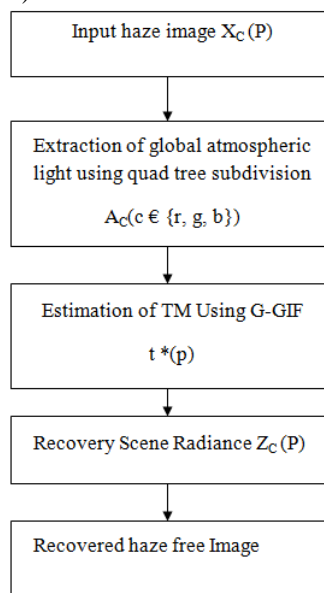


Figure 5: Flow Diagram of G-GIF

where $c \in \{r, g, b\}$ is a color channel index, X_c is a haze image, Z_c is a haze-free image, A_c is the global atmospheric light, and t is the medium transmission describing the portion of the light that is not scattered and reaches the camera.

Scene Radiance Recovery

The depth of the scene d and the atmospheric light A are known, and hence the medium transmission t can be estimated easily and recover the scene radiance J in Equation below,

$$J(x) = \frac{I(x)-A}{t(x)} + A = \frac{I(x)-A}{e^{-\beta d(x)}} A \text{ Equation(4.9)}$$

For avoiding producing too much noise, it is necessary to restrict the value of the transmission $t(x)$ between 0.1 and 0.9. So the final function used for restoring the scene radiance J in the proposed method can be expressed by:

$$J(x) = \frac{I(x)-A}{\min \{ \max \{ e^{-\beta d(x)}, 0.1 \}, 0.9 \}} + A \text{ Equation (4.10)}$$

The adaptive domain selection strategy can be organized to code each patch, which is called the difference-structure - preservation dictionary.

Simulation Results

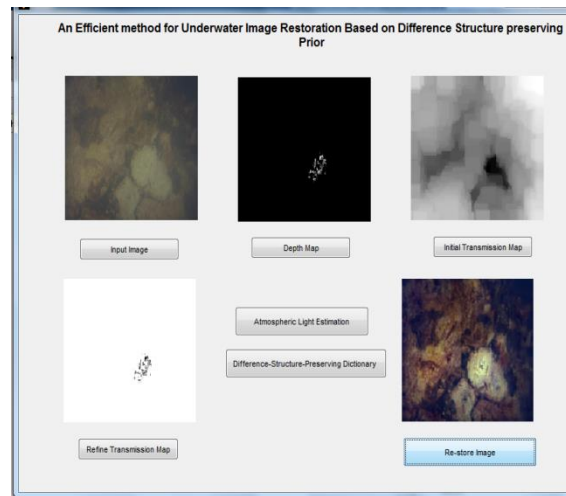


Figure 6: Simulation result of DSPV algorithm

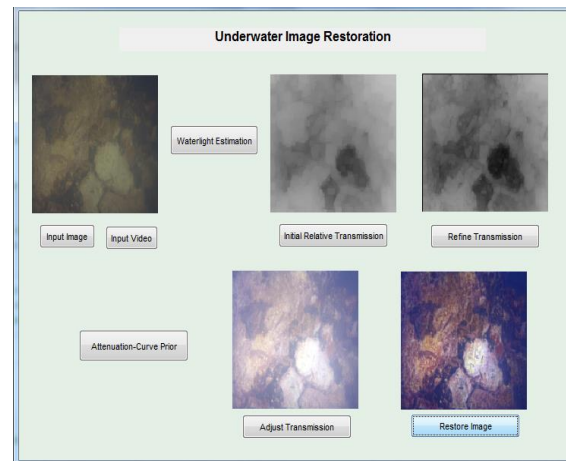


Figure 7: Simulation result of AACP

The proposed AACP method can generate more satisfactory restoration results. Furthermore, it can recover more red color because of the effect of attenuation factor estimation in this method. The result of this AACP method outperforms others in respect of the contrast and color correction.

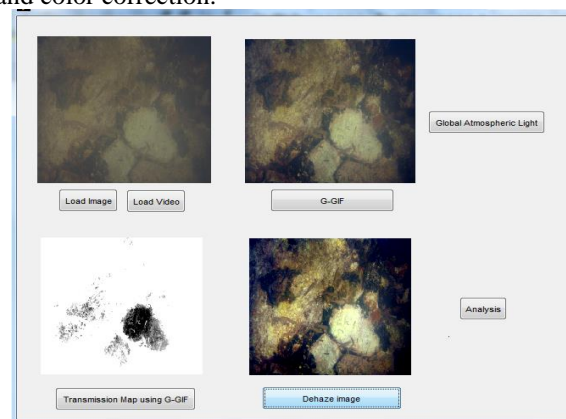


Figure 8: Simulation Result of G-GIF

Qualitative Comparison

Both the underwater images and videos are restored in a better manner using all these three algorithms. Also, a comparison has been made between these algorithms based on three parameters:

- Newly Visible Edges
- Mean ratio of Gradients
- White pixel ratio

For better understanding, a comparison has been made with five different images. The following chart shows the comparison of the mean ratio of gradient between the three proposed algorithms

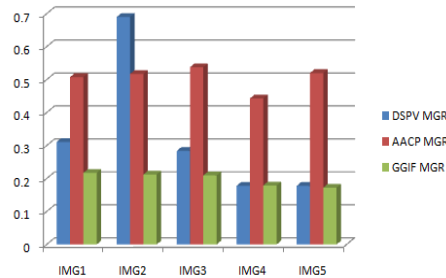


Figure 9: Comparison of three algorithms based on MGR

It is observed that the AACP algorithm shows the better result with all the five given input images. Meanwhile, the newly visible edges is more likely obtained using the DSPV algorithm.

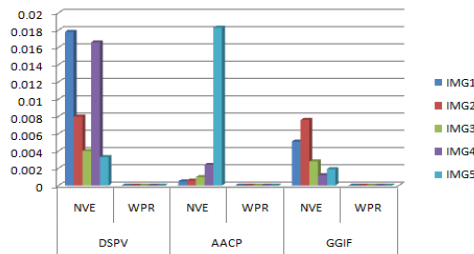


Figure 10: Comparison of three algorithms based on NVE and WPR

The above chart shows the comparison of the proposed algorithms based on the two parameters named as newly visible edges and white pixel ratio. The white pixel ratio of the well restored image must always be zero. In comparison, G-GIF method can recover and preserve the structures without sacrificing the fidelity of the color, such as with the swans in this image. More importantly, the result shown by G-GIF seems visually more reliable in distant regions.

These results achieve not only vivid color and better perception but also the best objective measurements. This demonstrates the success in terms of depth accuracy and the effectiveness of constraining both the smoothness and construct preservation. Therefore, it is observed that the G-GIF can suppress most of the artifacts that occur in the conventional dehazing algorithms.

IV CONCLUSION

This project analysed three underwater image and video restoration algorithms namely DSPV, AACP and G-GIF which can estimate the optimal transmission map and restore the actual scene. In DSPV method, in order to obtain the rough transmission map, two basic properties in the haze model are used to resolve the optimal parameter at the same depth. It is concluded that all the three methods are performed well in enhancing the underwater images as well as videos. Experimental test results were also used to verify the true representation of the methods. By this extend DSPV outperforms among these three.

V FUTURE ENHANCEMENT

For real-time scenarios, maybe we have sacrificed a little image restoration quality to improve the efficiency. So, it increases the efficiency some intelligent machine learning algorithms such as the deep learning algorithm can be introduced for image quality enhancement. There are no effective video defogging algorithms are available with desirable efficiency. We could analysis the few more methods based on the efficiency as the major constrain in future, which lead us to point out the procedure which easily enhances the underwater images in real-time live streaming scenario.

REFERENCES

1. P. Drews, E. do Nascimento (2013), "Transmission Estimation in Underwater Single Images", Computer Vision Workshops, IEEE International Conference on Computer vision workshop.
2. Hung-Yu Yang, Pei-Yin Chen (2011), "Low Complexity Underwater Image Enhancement Based on Dark Channel Prior", Second International Conference on Innovations in Bio-inspired Computing and Applications.
3. Linyuan He, Jizhong Zhao (2016), "Haze Removal using the Difference-Structure-Preservation Prior", Image Processing, IEEE Transactions on, DOI 10.1109/TIP.2016.2644267.



4. Yan-TsungPeng, Xiangyun Zhao and Pamela C. Cosman (2015), “Single Underwater Image Enhancement Using Depth Estimation Based On Blurriness”, National Science Foundation under Grant CCF-1160832.
5. Yi Wang (2017), “Single Underwater Image Restoration Using Adaptive Attenuation-Curve Prior”,Circuits and Systems,IEEE Transactions on,1549-8328 © 2017 IEEE.
6. Zhengguo Li (2018), “Single Image De-Hazing Using Globally Guided Image Filtering”,Image Processing, IEEE Transactions on,1057-7149 © 2017 IEEE.
7. K. He, J. Sun, and X. Tang. Single image haze removal using dark channel prior. In IEEE CVPR, pages 1956–1963, 2009.
8. C. Ancuti, C. Ancuti, T. Haber, and P. Bekaert. Enhancing underwater images and videos by fusion. In IEEE CVPR, pages 81–88, 2012.
9. N. Carlevaris-Bianco, A. Mohan, and R. Eustice. Initial results in underwater single image dehazing. In IEEE OCEANS, pages 1–8,2010.